

Ferroelectric ceramics in a pyroelectric accelerator

A. V. Shchagin¹, V. S. Miroshnik, V. I. Volkov, and A. N. Oleinik

Citation: *Appl. Phys. Lett.* **107**, 233505 (2015); doi: 10.1063/1.4937007

View online: <http://dx.doi.org/10.1063/1.4937007>

View Table of Contents: <http://aip.scitation.org/toc/apl/107/23>

Published by the [American Institute of Physics](#)



CiSE magazine is
an innovative blend.

COMPUTING

ENGINEERING

SCIENCE

Computing
- SCIENCE - ENGINEERING
EXPLORING OUR
SOLAR SYSTEM

Ferroelectric ceramics in a pyroelectric accelerator

A. V. Shchagin,^{1,2,a)} V. S. Miroshnik,¹ V. I. Volkov,¹ and A. N. Oleinik²

¹Kharkov Institute of Physics and Technology, Kharkov 61108, Ukraine

²Belgorod State University, Belgorod 308015, Russia

(Received 4 September 2015; accepted 22 November 2015; published online 9 December 2015)

The applicability of polarized ferroelectric ceramics as a pyroelectric in a pyroelectric accelerator is shown by experiments. The spectra of X-ray radiation of energy up to tens of keV, generated by accelerated electrons, have been measured on heating and cooling of the ceramics in vacuum. It is suggested that curved layers of polarized ferroelectric ceramics be used as elements of ceramic pyroelectric accelerators. Besides, nanotubes and nanowires manufactured from ferroelectric ceramics are proposed for the use in nanometer-scale ceramic pyroelectric nanoaccelerators for future applications in nanotechnologies. © 2015 AIP Publishing LLC.

[<http://dx.doi.org/10.1063/1.4937007>]

It has been known that pyroelectric crystals can emit electrons of energy up to tens of keV at heating and cooling in vacuum.^{1–3} In Ref. 4, the generation of X-ray radiation by electrons produced in the accelerator based on the pyroelectric crystal has been shown by an experiment. These facts stimulated the development of numerous studies on application of pyroelectric crystals such as LiNbO₃ and LiTaO₃ for acceleration of electron/ion beams in miniature (cm-scale size) pyroelectric accelerators. Now, these accelerators are used for acceleration of self-focused electron beam with near-equidistant spectrum, generation of X-ray radiation of energy up to ~100 keV and higher,^{3–11} production of 2.45 MeV neutrons in the D + D reaction,^{12–14} and also for electron-beam irradiation of materials.¹⁵ Some of the related theoretical research and studies of photogalvanic effect can be found in Refs. 16 and 17. In the present paper, we describe the experimentation on the applicability of ferroelectric ceramics as a pyroelectric in the pyroelectric accelerator, and the observation of X-rays produced by electrons accelerated in this ceramic accelerator.

Experiments have been performed at the Kharkov Institute of Physics and Technology, Ukraine. The scheme of the experimental setup is shown in Fig. 1. The pyroelectric accelerator is inside the cylindrical vacuum chamber V made of stainless steel. The inner diameter of the chamber is 250 mm, its height is 300 mm. The chamber is evacuated by a mechanical fore-vacuum pump through a nitrogen trap. The residual gas pressure in the chamber can be smoothly regulated by a flow control device. The pressure is measured by a thermocouple vacuum gage. The ferroelectric ceramics cylinder F is glued to the end of the grounded heat-conductor H installed along the axis of the chamber. The free end of the cylinder faces the beryllium window W of the X-ray detector D. The opposite end of the heat-conductor is immersed into liquid nitrogen N outside the chamber. The ferroelectric ceramics may be heated as the electric current passes from an outer source through the glassed-in resistor R located on

the heat-conductor. The temperature is measured in the vicinity of the ferroelectric ceramics by the thermocouple T.

The X-ray radiation spectra were measured with the spectrometer that consists of the 5 × 5 × 1 mm CdTe X-ray detector Amptek XR-100T and a digital pulse processor PX-4 connected to the computer. The 100 μm thick Be entrance window of the detector was sunk into the vacuum chamber. The distance between the Be window and the free end of the ferroelectric ceramics was 20 mm. The X-ray spectrometer was energy calibrated with the use of radioactive sources ⁵⁵Fe and ²⁴¹Am. The energy resolution of the X-ray spectrometer was 300 eV at X-ray energy of 5.9 keV.

In our trial experiments, the main objective was to observe X-rays using the samples of modified lead-calcium titanate ferroelectric ceramics. Usually, it is used as a pyroelectric. The samples were shaped as disks of diameter 9 mm and thickness 0.43 mm, and were polarized along the disk

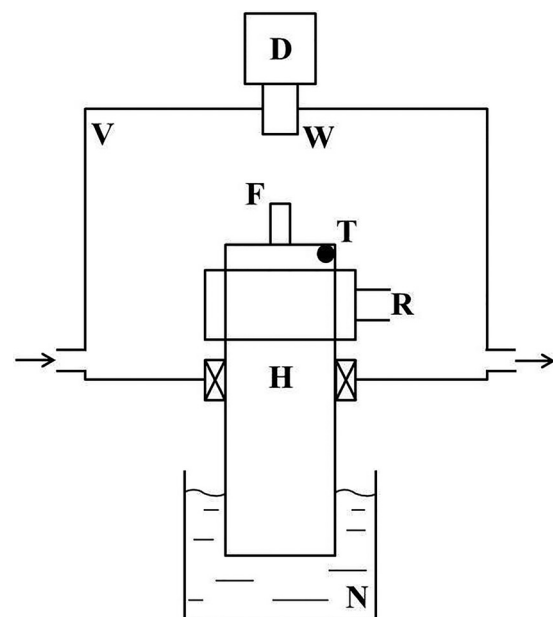


FIG. 1. Scheme of the experimental setup. D—X-ray detector with beryllium entrance window W; V—vacuum chamber; F—ferroelectric ceramics; T—thermocouple; H—copper heat-conductor; R—heating resistor; N—liquid nitrogen.

^{a)} Author to whom correspondence should be addressed. Electronic mail: shchagin@kipt.kharkov.ua. On leave from Laboratoire de l'Accélérateur Linéaire, Centre Scientifique d'Orsay Bâtiment 200 - BP 34 91898 Orsay cedex - France

axis. Both the disk faces were coated with silver. Stacks of 1, 2, 4 disks, connected in series, were heated and cooled in the chamber at different residual gas pressures; however, no X-rays were detected.

In the present experiments, we observed the X-rays using lead barium zirconate titanate ferroelectric ceramics. Usually, it is used as a piezoelectric, but we have made use of its pyroelectric properties. The ceramics was produced in the form of cylinders with diameter 6.4 mm and length 15 mm, and was polarized along the cylinder axis. In our experiments, we have used the cylinders of lengths $L = 15$ and 30 mm. The 30 mm cylinder was made by gluing together two series-connected 15 mm cylinders with the use of electrically conductive epoxy. The cylinders were arranged in the vacuum chamber in two alignments to provide the positive charge at the free end of the cylinder at heating (“-” alignment), or at cooling (“+” alignment). The cylinders were glued to the ferrule of the heat-conductor by electrically conductive epoxy. The alignments are marked by the signs in Figs. 2 and 3.

No X-ray radiation was observed when ceramics was at constant temperature. All the spectra described below were measured during ceramics heating or cooling. The duration of heating from $-50\text{ }^{\circ}\text{C}$ to $+85\text{ }^{\circ}\text{C}$ was about 15 min, and the duration of cooling from $+85\text{ }^{\circ}\text{C}$ to $-50\text{ }^{\circ}\text{C}$ was about 30 min until the temperature stabilization. Some of the measured X-ray spectra are shown in Figs. 2 and 3. The spectra

were measured at several residual gas (air) pressure (P) values, using ferroelectric ceramics of length $L = 15$ mm in the “-” alignment, and $L = 30$ mm in the “+” alignment. The ceramics length and alignment as well as the pressure values for every spectrum are given in Figs. 2 and 3.

The positive charge arises at the free end of the ferroelectric ceramics due to the pyroelectric effect at heating (Figs. 2(a) and 2(c)) in the “-” alignment, and cooling (Figs. 3(a) and 3(c)) in the “+” alignment of the ceramics. Electrons from the residual gas are accelerated in the electric field and strike the ferroelectric ceramics surface. The bremsstrahlung and characteristic X-ray radiation result from the interaction of the electrons with atoms composing the ceramics. One can see spectral peaks of characteristic X-ray radiation against the smooth background of the bremsstrahlung in the spectra. The spectral peak at energy 2.3 keV corresponds to M_{α} lines of Pb. The peak at energy of 4.5 keV corresponds to K_{α} lines of Ti and L_{α} lines of Ba. The peak at energy 8.5 keV may be due to L_{α} lines of Re. The peaks at energies 9.2, 10.5, 12.6, 14.8 keV are due to $L_{1}, L_{\alpha}, L_{\beta}, L_{\gamma}$ lines of Pb, respectively; the peaks at energies of 15.8 and 17.7 keV are due to K_{α} and K_{β} lines of Zr. The spectral peaks of K-radiation of Ba, Re and Pb are not seen because of restricted energy of the accelerated electrons and/or a low radiation yield.

The negative charge arises at the free end of the ferroelectric ceramics due to the pyroelectric effect at cooling (Figs. 2(b) and 2(d)) in the “+” alignment, and heating

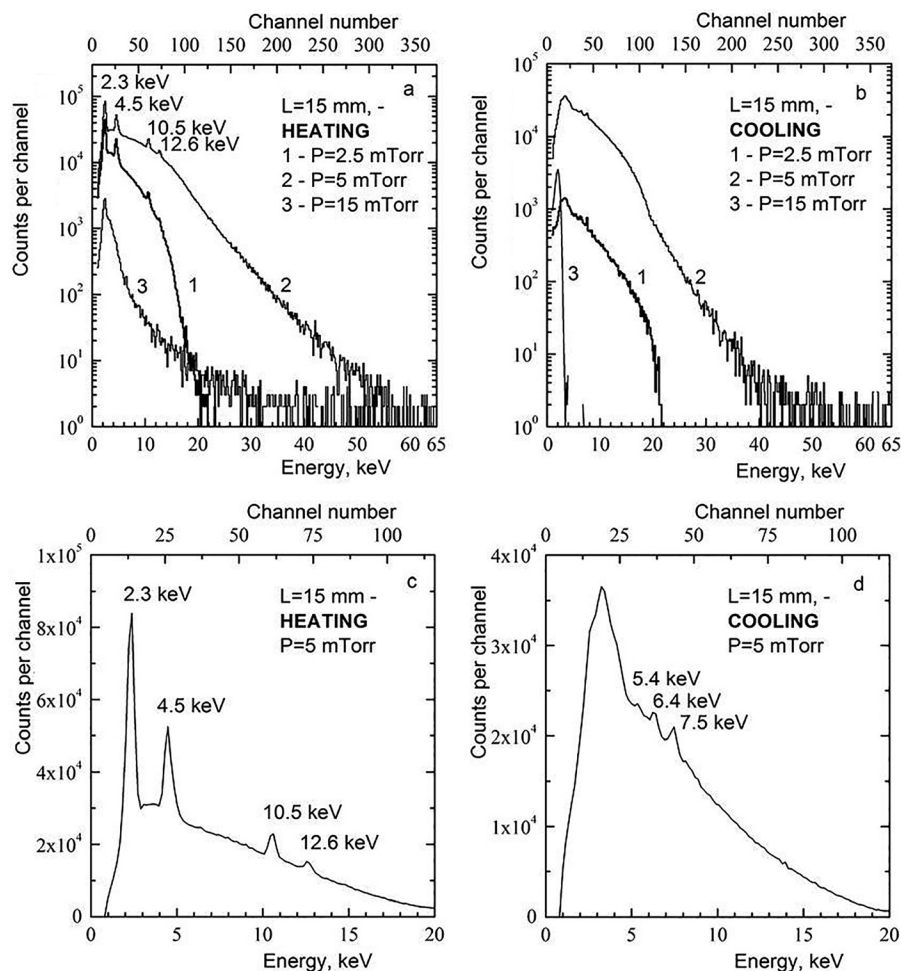


FIG. 2. X-ray spectra measured during one heating (a) - cooling (b) cycle for ferroelectric ceramics of length $L = 15$ mm in “-” alignment on a logarithmic scale. The low-energy parts of the spectra ((a) and (b)) at $P = 5$ mTorr are also shown on a linear scale in Figs. (c) and (d), respectively.

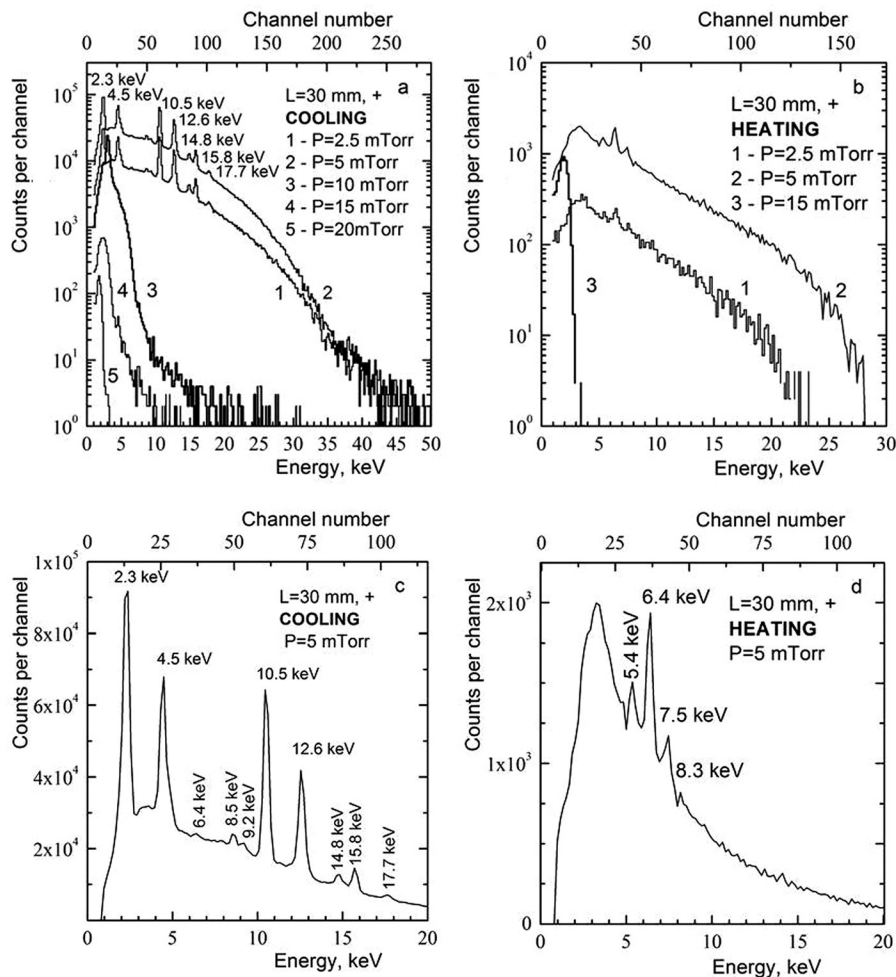


FIG. 3. The same as in Fig. 2 but for the ferroelectric ceramics of length $L = 30$ mm in “+” alignment.

(Figs. 3(b) and 3(d)) in the “–” alignment of the ceramics. Electrons from the ferroelectric ceramics surface are accelerated in the electric field and strike the Be window of the detector and the stainless steel chamber walls. The bremsstrahlung and characteristic X-ray radiation from the atoms composing the stainless steel are emitted at deceleration of the electrons in the window and walls. The spectra show the peaks of characteristic X-ray radiation against the smooth background of the bremsstrahlung. The spectral peaks at energies of 5.4, 6.4, 7.5 keV are due to K_{α} -lines of the atoms Cr, Fe, Ni in the stainless steel, respectively, and the peak at energy of 8.3 keV is due to K_{β} -line of Ni.

One might expect the maximum energy and yield of the radiation to increase with an increase in the ferroelectric cylinder length. However, these expectations lack support from the measurements, which show that in some cases the maximum energy and yield are even higher for a shorter cylinder, see Figs. 2 and 3. This could be due to different temperature distributions in the short and glued long cylinders. The maximum energy of the observed bremsstrahlung exceeds 50 keV at $P = 5$ mTorr. This means that it is contributed by the electrons accelerated in the ceramic accelerator up to the energy exceeding 50 keV. It can be seen from Figs. 2 and 3 that the maximum energy of bremsstrahlung and accelerated electrons, as well as the total number of counts in the spectra, appreciably change with variation in the pressure in the mTorr range. Note that the pyroelectric accelerators based

on pyroelectric crystals usually work in the same pressure range. A more detailed research of the pressure dependences will be presented elsewhere.

Our experimental research has demonstrated that instead of pyroelectric crystals, ferroelectric ceramics can be used in a pyroelectric accelerator. The appearance of a high potential on the ferroelectric ceramics surface may be caused by the classical pyroelectric effect, and also, by the so-called tertiary pyroelectric effect. The tertiary pyroelectric effect can be due to the mechanical strength of the ceramics that can arise at nonuniform heating or cooling along the ceramics cylinder. The mechanical strength can give rise to the piezoelectric effect in addition to the classical pyroelectric effect.

The maximum X-ray energy observed in the present work is lower than that attained with the use of pyroelectric crystals. To clear up the capabilities of the pyroelectric accelerators based on ferroelectric ceramics and compare them to the ones achieved with crystalline pyroelectrics, one should perform experimental research into the accelerator properties with the use of different kinds of ferroelectric ceramics and select the best of them.

Let us discuss some prospects for application of ferroelectric ceramics in pyroelectric accelerators. Unlike pyroelectric crystals, ferroelectric ceramics can be produced in arbitrary shape and be polarized in arbitrary directions. Therefore, various shaped ceramic elements can be used in

pyroelectric accelerator designs. For instance, spherical or cylindrical layers of radially polarized ceramics can be used for creation of the pyroelectric accelerator of spherical or cylindrical shape. Probably, such spherical or cylindrical accelerators can provide higher beam energy and current in comparison with the flat accelerators now in use. Besides, deuterium residual gas can usefully be applied for generation of X-rays, because it shows the best efficiency for production of X-ray radiation with the crystalline pyroelectric when compared to some other gases.¹⁰

Note also the potential for further miniaturization of the pyroelectric accelerator. At present, the size of pyroelectric accelerators is of cm scale. Recently, nanoshell tubes and nanowires of ferroelectric ceramics have been developed, see, e.g., Refs. 18 and 19. The nanoshell tubes and nanowires made from ferroelectric ceramics can be used in the structure of a miniature pyroelectric accelerator of nanometer-scale size. Such a nanoaccelerator of low energy electrons and ions can find applications in nanotechnologies.

A.V.S. is thankful to F. Goennenwein for preliminary stimulating discussions about experimental research of pyroelectric accelerator based on ferroelectric ceramics. The authors are thankful to V. I. Nagaychenko for conducting the most of experimental measurements. This paper was partially supported by the Grant No. 1911 from the Science and Technology Center in Ukraine, by the Ministry of Education and Science of the Russian Federation under Project No. 3.2009.2014/K, and the Foundation for Assistance to Small Innovative Enterprises (Russia), Project No. 0002356\2014.

- ¹B. Rosenblum, P. Braunlich, and J. P. Carrico, *Appl. Phys. Lett.* **25**, 17 (1974).
- ²G. Rosenman and I. Rez, *J. Appl. Phys.* **73**, 1904 (1993).
- ³G. Rosenman, D. Shur, Ya. E. Krasik, and A. Dunaevsky, *J. Appl. Phys.* **88**, 6109 (2000).
- ⁴J. D. Brownridge, *Nature* **358**, 287 (1992).
- ⁵J. D. Brownridge and S. Raboy, *J. Appl. Phys.* **86**, 640 (1999).
- ⁶J. D. Brownridge and S. M. Shafroth, *Appl. Phys. Lett.* **79**, 3364 (2001).
- ⁷J. D. Brownridge and S. M. Shafroth, *Trends in Lasers and Electro-Optics Research* (Nova Science, New York, 2004), p. 57.
- ⁸See <http://www.amptek.com/coolx.html> for Amptek Inc., Miniature X-ray generator with pyroelectric crystal.
- ⁹V. I. Nagaychenko, V. V. Sotnikov, B. I. Ivanov, A. M. Yegorov, and A. V. Shchagin, *Problems of Atomic Science and Technology, Ser. Plasma Electronics and New Methods of Acceleration* **5**, 254 (2006) (in Russian).
- ¹⁰V. I. Nagaichenko, V. A. Voronko, V. V. Sotnikov, V. V. Sidorenko, P. S. Kizim, A. M. Yegorov, and A. V. Shchagin, *Problems of Atomic Science and Technology, Ser. Nuclear Physics Investigations* **50**, 72 (2008) (in Russian).
- ¹¹V. I. Nagaychenko, V. V. Sotnikov, B. I. Ivanov, A. M. Yegorov, and A. V. Shchagin, *J. Surf. Invest.: X-ray, Synchrotron Neutron Tech.* **3**, 81 (2007) (in Russian).
- ¹²B. Naranjo, J. K. Gimzewski, and S. Putterman, *Nature* **434**, 1115 (2005).
- ¹³J. Geuther, Ya. Danon, and F. Saglime, *Phys. Rev. Lett.* **96**, 054803 (2006).
- ¹⁴D. Gillich, A. Kovanen, B. Herman, T. Fullem, and Ya. Danon, *Nucl. Instrum. Methods A* **602**, 306 (2009).
- ¹⁵J. Geuther and Ya. Danon, *Nucl. Instrum. Methods B* **261**, 110 (2007).
- ¹⁶N. Kukhtarev, J. D. T. Kukhtareva, M. Bayisse, J. Wang, and J. D. Brownridge, *J. Appl. Phys.* **96**, 6794 (2004).
- ¹⁷N. V. Kukhtarev, T. V. Kukhtareva, G. Stargell, and J. C. Wang, *J. Appl. Phys.* **106**, 014111 (2009).
- ¹⁸Y. Luo, I. Szafraniak, N. D. Zakharov, V. Nagarajan, M. Steinhart, R. B. Wehrspohn, J. H. Wendorff, R. Ramesh, and M. Alexe, *Appl. Phys. Lett.* **83**, 440 (2003).
- ¹⁹J. Wang, C. S. Sandu, E. Colla, Y. Wang, W. Ma, R. Gysel, H. J. Trodahl, N. Setter, and M. Kuball, *Appl. Phys. Lett.* **90**, 133107 (2007).